Available online at www.sciencedirect.com
SCIENCE DIRECT®
Journal of Theoretical Biology 222 (2003) 9–22
Journal of Theoretical Biology
www.elsevier.com/locate/jtbi

A spatial model of germinal center reactions: cellular adhesion based sorting of B cells results in efficient affinity maturation

Can Keşmir*, Rob J. De Boer

Department of Theoretical Biology, Utrecht University, Padualaan 8, 3584-CH, Utrecht, The Netherlands

Received 1 March 2001; accepted 7 June 2002

Abstract

Affinity maturation of humoral responses to T-cell-dependent antigens occurs in germinal centers (GC). In GCs antigen-specific B cells undergo rounds of somatic mutations that alter their affinity. High-affinity mutants take over GCs very soon after they appear; the replacement rate is as high as 4 per day (Radmacher et al., Immunol. Cell Biol. 76 (1998) 373). To gain more insight into this selection process, we present a spatial model of GC reactions, where B cells compete for survival signals from follicular dendritic cells (FDC). Assuming that high-affinity B cells have increased cellular adhesion to FDCs, we obtain an affinity-based sorting of B cells on the FDC. This sorting imposes a very strong selection and therefore results in a *winner-takes-all* behavior. By comparing our sorting model with "affinity-proportional selection models", we show that this *winner-takes-all* selection is in fact required to account for the fast rates at which high affinity mutants take over GCs. Another important feature of *in vivo* GC reactions is that they are non-mixed, i.e. GCs contain either no high-affinity cells at all or they are dominated by high-affinity cells. We here show that this *all-or-none* behavior can be obtained if B cells are sorted based on their affinity on the FDC surface. Affinity-proportional selection models, in contrast, always produce mixed GCs.

Keywords: Germinal center reactions; Affinity maturation; Cellular adhesion; Spatial model

1. Introduction

The antibody response to T-cell-dependent antigens matures in germinal centers (MacLennan, 1994) where B cells undergo extensive proliferation and differentiation (Liu and Banchereau, 1997; Liu et al., 1991; Tarlinton, 1998). The GC environment provides signals to the B cells, causing them to switch on a hypermutation mechanism that alters their affinity (Betz et al., 1993; Kelsoe, 1999; Klein et al., 1998; Wabl et al., 1999; Wiens et al., 1998; Yelamos et al., 1995). The high mutation rate amounts to roughly 10^{-3} per base pair per division (Berek and Milstein, 1987), i.e. each B cell is expected to produce approximately one mutant per cell division. Under such conditions, a high-affinity clone would suffer from mutational decay unless it is subject to very strong selection. Selection takes place in two stages. First, mutated B cells compete for antigen bound to FDCs (Kelsoe, 1996; Przylepa et al., 1998). Second, they compete for T cell help (Choe et al., 2000; Lindhout et al., 1997; Manser et al., 1998; Yellin et al., 1994). The strong selection in GCs results in an *all-or-none* behavior: GCs either contain hardly any high-affinity cells, or they are almost completely taken over by high-affinity mutants (Berek et al., 1991; Radmacher et al., 1998). The conventional model for the replacement of mutants by selection is

$$\frac{d\rho}{dt} = k\rho(1-\rho), \tag{1}$$

where ρ is the fraction of a high-affinity mutant, and k is the growth/replacement rate (Maree et al., 2000). Radmacher et al. calculated the growth/replacement rate of a high-affinity mutant (with ten-fold increased affinity) to be almost 4 per day (Radmacher et al., 1998). Since the estimated maximum proliferation rate of GC B cells is also 4 per day (Liu et al., 1991), the growth rate (or fitness) of the germ line B cells (i.e. the B cells that carry germ line encoded immunoglobulin) seems to drop to zero when the first high-affinity mutants appear. That

*Corresponding author. Tel.: +31-30-2533-637; fax: +31-30-251-3655.
E-mail address: c.kesmir@bio.uu.nl (C. Keşmir).

0022-5193/03/$ - see front matter © 2003 Elsevier Science Ltd. All rights reserved.
doi:10.1016/S0022-5193(03)00010-9

is, high-affinity mutants would either need to proliferate unrealistically fast, or their death rate would need to be several fold lower than that of germ line B cells. We can make this argumentation more precise by developing a general affinity proportional selection model.

1.1. A general affinity-proportional selection model

Consider an established GC with a steady-state B-cell population B_0 proliferating at an estimated rate of approximately four divisions per day. The B_0 cells are considered to be the germ line B cells that have not yet accumulated any mutations increasing their affinity. The B_0 cells have an affinity K_0 that influences their proliferation rate, and/or their survival. The stable steady-state population size in the GC is brought about by competition between the B cells, which may decrease the proliferation rate, and/or the survival rate. We will consider classes of B cells B_i with an increased affinity K_i for the relevant antigen. Let B_1 be the first clone with increased affinity, B_2 be superior to B_1, and so on.

First, consider a model where the proliferation rate increases with the affinity and decreases with the total population size T, and the death rate is independent of affinity and may increase with the total population size, i.e.

$$\frac{dB_i}{dt} = [\rho(K_i, T) - \delta(T)]B_i, \tag{2}$$

where $\partial\rho(K_i,T)/\partial K_i > 0$, $\partial\rho(K_i,T)/\partial T < 0$, and $\partial\delta(T)/\partial T > 0$. When the germ line B cells approach steady state they should proliferate at a rate $\rho(K_0,T) = \delta(T) \simeq 4$ per day, with $T = B_0$. When the first higher affinity mutants appear, i.e. when $B_1 = 1$, they are proliferating at a faster rate $\rho(K_1,T)$ and dying at the same rate $\delta(T)$, with $T \simeq B_0$. Since, we consider the case where B_0 cells and mutants differ only in their proliferation rate, we can substitute $\delta(T) = \rho(K_0,T)$ to obtain

$$\frac{dB_1}{dt} \simeq [\rho(K_1, T) - \rho(K_0, T)B_1]. \tag{3}$$

Hence the mutant expands at a rate defined by the difference in the proliferation rates: a well-known result of population genetics (Maree et al., 2000). The observed replacement rate of 4 per day therefore requires that $\rho(K_1,T) \simeq 8$ per day, which is unrealistically fast. Moreover, if the next mutant with further increased affinity were also to take over at a rate of 4 per day, it would need to have $\rho(K_2,T) \simeq 12$ per day, which is even more unrealistic. This is a general result because we have not specified the precise form of the competitive proliferation and death functions. The result is also conservative: if the total population size were to increase during affinity maturation, it would become even more difficult to obtain such large increases in the proliferation rates, since competition increases with the population size, T.

As an alternative model, assume that the affinity determines the death/survival rates:

$$\frac{dB_i}{dt} = (\rho(T) - \delta(K_i, T))B_i, \tag{4}$$

where $\partial\rho(T)/\partial T < 0$, $\partial\delta(K_i,T)/\partial K_i < 0$, and $\partial\delta(K_i,T)/\partial T > 0$. If the first mutant B cells appear when the germ line B cells have approached steady state, i.e. when $\rho(T) = \delta(K_0,T) \simeq 4$ per day with $T = B_0$, one obtains

$$\frac{dB_1}{dt} = [\delta(K_0, T) - \delta(K_1, T)]B_1, \tag{5}$$

which implies that the first mutant expands at a rate defined by the difference in the death rates. To obtain a replacement rate of 4 per day with $\delta(K_0,T) \simeq 4$ per day (Cohen et al., 1992) one needs $\delta(K_1,T) \ll \delta(K_0,T)$. Thus, the average lifespan of the first mutants has to be say 10 times longer, which is again unrealistic. Moreover, one would expect a much larger new steady-state population size $T = B_1$ when the mutant has taken over. Again, this problem becomes worse when one considers the subsequent invasion of a B_2 population in a GC dominated by B_1 cells.

Thus, to explain the *in vivo* data, we need a mechanism that is not just proportional to the affinity, but reinforces the effect of the affinity. We investigate a possible new selection mechanism by replacing the assumption of affinity-proportional death or proliferation rates by affinity-based sorting of B cells on FDCs. We develop a spatial GC model in which B cells move, divide, mutate, and die. In this model B cells compete with each other for space (i.e. for survival signals) on the FDC surface. We obtain a spatial sorting of the B cells on the FDC, if we assume that B cells with increased affinity have an increased cellular adhesion to the FDC. This leads to a *winner-takes-all* selection because, by means of adhesion-based cellular sorting (Steinberg, 1970), only the highest affinity B cells will contact the FDC and be rescued. Such a *winner-takes-all* selection is no longer proportional to the affinity and can easily account for rapid replacement rates. The formalism used for our model was developed earlier for adhesion-based cell sorting (Glazier and Graner, 1993; Graner and Glazier, 1992), and is here extended with GC-specific cellular processes.

Many theoretical models of affinity maturation (Kepler and Perelson, 1993a, b; Oprea and Perelson, 1997; Oprea et al., 2000) are good at simulating the *average* affinity maturation. However, they are poor at explaining the rapid take-over of mutants, and the *all-or-none* behavior of individual GCs (Kleinstein and Singh, 2001), i.e. individual GCs are not mixtures of high- and low-affinity cells: they contain either only high-affinity B cells, or only low-affinity cells. The major reason for this is the affinity-proportional selection mechanism. We compare our model with previous models and show that with adhesion-based cellular

sorting, we obtain a much faster selection of high-affinity mutants.

2. Model

2.1. Biology of germinal centers

The primary humoral follicular immune response starts with the rapid expansion of 3–5 antigen-specific B cells (Jacob et al., 1991; Liu et al., 1991). Within 3 days B cell numbers exceed 10^3 cells. This rapid expansion is followed by differentiation: a certain fraction of blast cells (i.e. the centroblasts) remains in cell cycle, downregulates its surface immunoglobulin, and creates the dark zone of the GC. The remaining blast cells revert to a centrocyte phenotype (Liu et al., 1991), move to the opposite pole of the FDC network, re-express their surface immunoglobulin, and create the light zone.

Centrocytes do not proliferate, and die rapidly unless they are "rescued". Centrocytes receive the first survival signal when they form complexes with antigen on FDCs (Koopman et al., 1997). While dissociating from FDCs, the centrocytes take up some antigen, which is later presented to GC T cells to get the second (cognate) survival signal (Casamayor-Palleja et al., 1995; Koopman et al., 1997). A centrocyte is rescued if it receives survival signals both from the FDC and from T cells. A rescued centrocyte exits the light zone, and either circulates back to the dark zone, where it restarts centroblast proliferation, or it leaves the GC to become a memory or plasma cell. Indeed, recent data suggest that the memory B cell population is generated throughout the GC reaction (Ridderstad and Tarlinton, 1998). These basics of a GC reaction are illustrated in Fig. 1.

2.2. Basic principles of the model

To study the affinity maturation of humoral responses in GCs, we use a hybrid cellular automaton (CA) like the model introduced by Graner and Glazier (Glazier and Graner; 1993; Graner and Glazier, 1992) (see Appendix A). This model has been used extensively for simulating cell sorting (Mombach and Glazier, 1996; Mombach et al., 1995), morphogenesis (Hogeweg, 2000a, b) and for simulating all stages of *Dictyostelium discoideum* slugs (Jiang et al., 1998; Maree and Hogeweg, 2001; Maree et al., 1999; Savill and Hogeweg, 1997).

The space in which the GC simulations take place is a rectangular lattice of CA "sites". We here use a standard size of 50×50 sites. Each biological cell is simulated by a number of connected lattice sites. Lattice sites that are not part of a biological cell represent the medium in which the cells reside. A cell interacts with other cells and with the medium according to pre-defined rules, dependent on the cell type (e.g. centrocyte, centroblast, FDC, or memory). In Fig. 2, we show a sketch of the lattice, where two centrocytes with high (dark gray) and low (white) affinity are interacting with an FDC (light gray). During a single update of the CA, a randomly chosen lattice site at a cell boundary is replaced by a randomly chosen neighbor with a probability that depends on the change in surface energy that would be brought about by the update. Lattice sites inside a cell or inside the medium are never updated, because exchanging two sites within a cell would not change the state of the system. As in the original model (Glazier and Graner, 1993; Graner and Glazier, 1992), the surface energy is the sum of adhesion energies between cells of different types or the medium (e.g. J_{cc}, J_{fc}, J_{fm}, J_{cm} in Fig. 2, and see Appendix A). To keep cells close to their target volume, an extra volume constraint term is added to the surface energy calculations. In the original model, the target volume of a cell does not change with time, causing very fast cell growth when space is unlimited. To obtain slow cell growth, we set the target volume of a cell to a small value after cell division and when the actual volume of the cell reaches the target volume, the target volume is slightly increased (see also Hogeweg, 2000a). This process is repeated until the target volume reaches a pre-defined maximum. In this way, the difference between the actual cell volume and the target volume never becomes very large, and thus cells grow slowly even if there is an excess of space.

We further extend the original model by letting cell adhesion between centrocytes and the FDC depend on the affinity of centrocytes for the antigen on the FDCs (see Eqs. (A.1) and (A.2) in Appendix A). The shaded area in Fig. 2 shows the sites where affinity contributes to cell adhesion. The contribution of affinity to cell adhesion is independent of how many sites are in contact with the FDC, as long as a centrocyte has the minimum contact necessary to obtain survival signals. The adhesion energy to the FDC is proportional to a cell's affinity, i.e. it is more advantageous for a high-affinity cell to be in contact with the FDC than it is for a low-affinity cell. As a result, high-affinity centrocytes tend to replace low-affinity centrocytes on the FDC surface. Thus, the chance that a low-affinity centrocyte will come into contact with the FDC decreases with the number of high-affinity centrocytes that are around. In Fig. 3, we show a series of snap-shots from a simulation to demonstrate the affinity-based cell sorting around the FDC. Note that the affinity only affects the adhesion of the centrocyte to the FDC and not, as in the conventional models, the lifespan of the various cell types or the effect of survival signals upon the centrocytes.

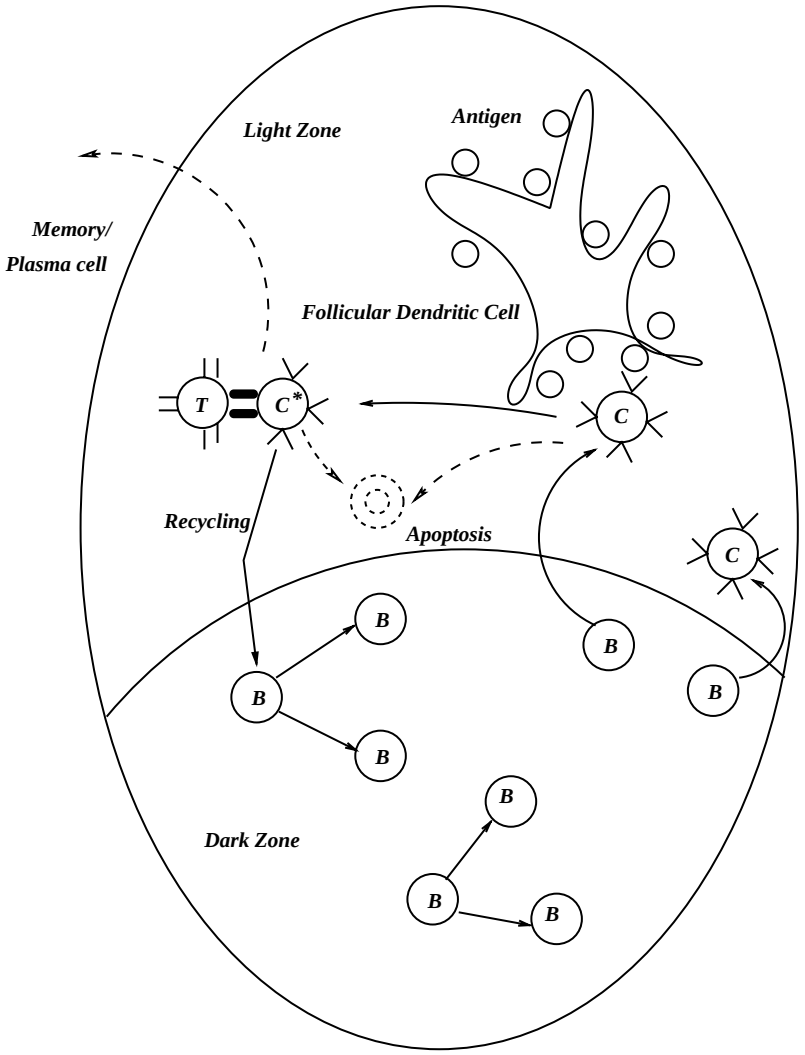

Fig. 1. A simplified scheme of GC reactions. The reaction starts with a few seeder cells of centroblast phenotype, *B*. After a certain number of cell divisions centroblasts differentiate to centrocytes, *C*. Interaction with antigen on FDCs is the first stage in centrocyte selection. Centrocytes that can bind antigen are rescued, whereas those that fail to bind antigen die by apoptosis. The second stage of selection involves a cognate interaction with GC T cells. Antigen-presenting centrocytes, C^*, that fail to make a cognate interaction with a GC T cell also die by apoptosis. The remaining cells either regain the centroblast phenotype (*B*), or leave the GC to populate the memory or the antibody-forming cell compartment.

2.3. Cellular processes implemented in the model

Simulations start with 6–8 seeder centroblasts and a single FDC that does not divide. Before a centroblast can divide it has to grow to a certain fixed volume. The number of cell divisions depends on the availability of empty space. This enforces a density-dependent growth resulting in a stable size of the GC. Cell division is implemented by dividing the area occupied by a cell into two, along the longest dimension. Each of the new cells get a unique identifier. A centroblast becomes a centrocyte when it reaches the end of its lifespan (see below).

Centrocytes need to interact with the FDC to be "rescued" from programmed cell death. We implement a chemotactic gradient, e.g. generated by B-cell-attracting chemokine BCA-1 (Legler et al., 1998), towards the FDC. This chemotactic gradient helps the centrocytes to find the FDC. Centrocytes compete with each other to gain access to the FDC surface. Once the centrocytes establish an FDC contact area covering more than three lattice sites, they start receiving survival signals. A centrocyte is rescued after it has accumulated a certain amount of survival signals, i.e. after being in contact with the FDC for a minimum amount of time. If a centrocyte fails to accumulate enough survival signals it dies via apoptosis. With a certain probability, p_r, a rescued centrocyte reverts to the centroblast phenotype. Otherwise it becomes a memory cell. The phenotype change occurs immediately after the centrocyte has accumulated enough survival signals. Because only centrocytes have a strong adhesion to the FDC

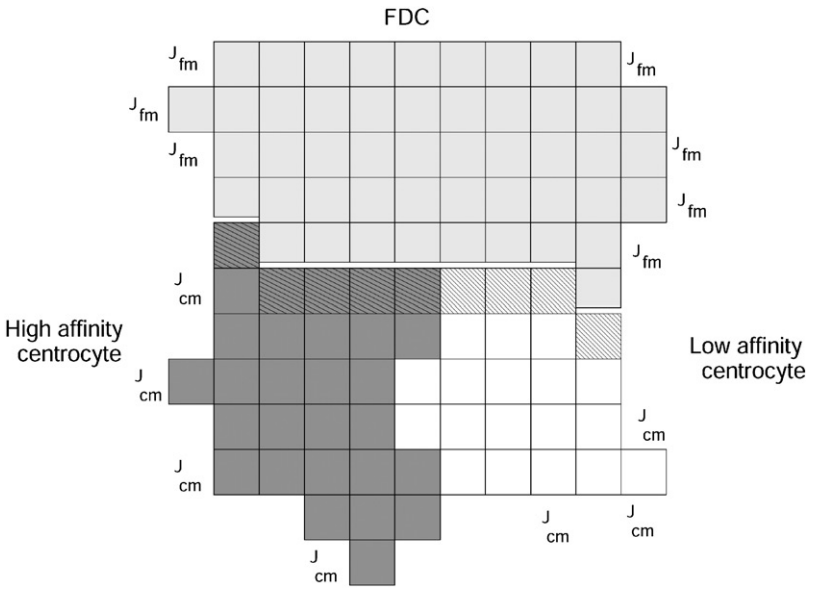

Fig. 2. A sketch of the model formalism. The dark gray and white cells are high- and low-affinity centrocytes, respectively. The light gray cell is the FDC. J values correspond to the different free energy bonds between cells and the medium. For each lattice site that is in contact with the medium or another cell, there is a corresponding J value. In the figure, we have depicted only some of the J values: J_{cc} between two centrocytes, J_{fc} between a centrocyte and FDC, J_{fm} between FDC and the medium and J_{cm} between a centrocyte and the medium. The affinity of a centrocyte influences its adhesion only in the FDC contact area (shaded).

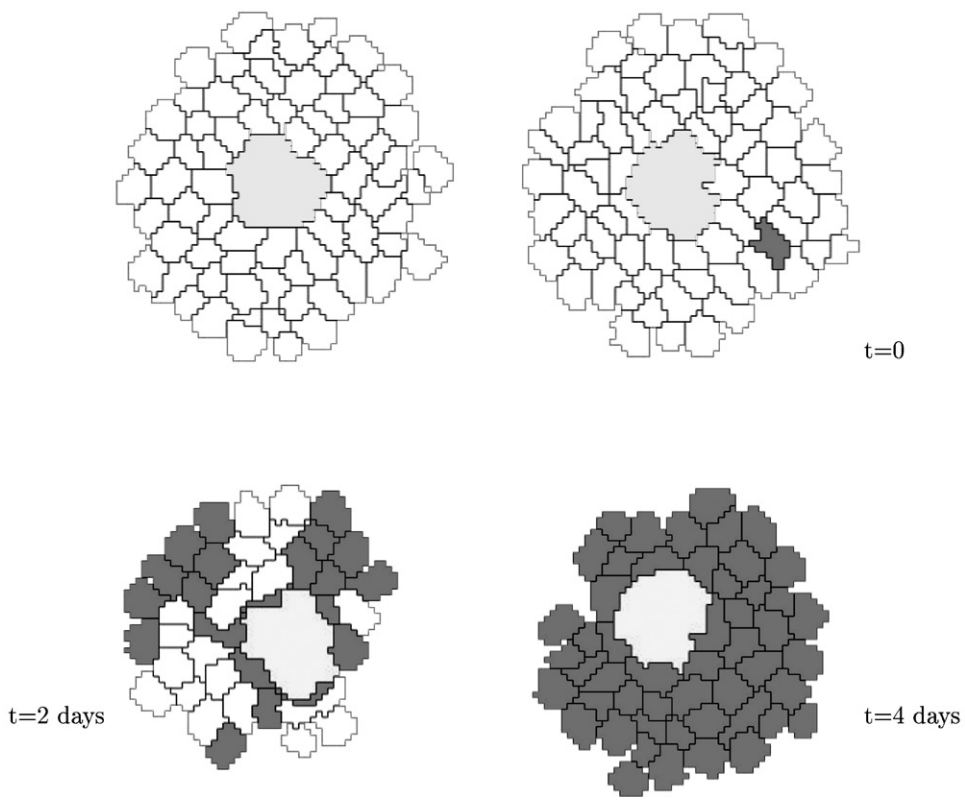

Fig. 3. A series of snap-shots from simulations. The first picture shows a GC populated by low-affinity cells (white). At $t=0$ a high-affinity mutant is introduced (dark gray cell). At the end of the second day, half of the cells are of high affinity, and the FDC (light gray cell) is largely covered by high-affinity cells. This panel represents the typical affinity-based sorting around the FDC. After 4 days the high-affinity B cells dominate the GC reaction.

(Pals et al., 1998), they dissociate from the FDC upon changing their phenotype. Centrocytes can also dissociate from the FDC without changing their phenotype, if they are "pushed away" by higher affinity centrocytes due to cellular sorting. If a centrocyte becomes a memory cell, it rapidly leaves the GC. In our simulations, memory cells are repelled by the chemotactic signals secreted by the FDC. Thus, a memory cell has little influence on our GC dynamics.

The age of the cells is implemented as a clock, which is synchronized with the simulation time steps. The actual age of a cell is the difference between the present simulation time step and the time step the cell was generated. When a cell changes its phenotype, its age is "reset", i.e. the actual simulation time step is recorded as the generation time of the cell. This resetting of age is necessary to give enough time to centrocytes to interact with the FDC and to centroblasts to generate offspring. When a cell divides, the generation time of the daughter cells is set to that of the parent cell. This prevents infinite division in the centroblast compartment without selection (see above). In order to avoid synchronized behavior in the model, i.e. to avoid having many cells with the same age and thus dying or differentiating at exactly the same time, we add noise to the generation times of the cells. This noise is distributed uniformly between –30% and +30% of the standard lifespan of the cell type, and added when the cells change their phenotype and/or divide. The distribution of realized lifespans for centrocytes (open bars) and centroblasts (filled bars) is given for a typical simulation in Fig. 4. While in contact with FDC, centrocytes are probably not sensitive to apoptosis. Thus, in the simulations we stop aging process when a centrocyte is in contact with the FDC. This hardly results in very long lifespans, as few centrocytes live more than 9 h (see Fig. 4).

A B cell's affinity for the antigen can change by somatic mutation. We group B cells (both centrocytes and centroblasts) into a small number of affinity classes, where all cells in affinity class i have similar affinity for the antigen. Germ line antigen-specific B cells are in affinity class 0. Somatic mutation is implemented as a stochastic process during cell division. Following a mutation, a B cell from affinity class i can either switch to class $i+1$, i.e. achieve a higher affinity or switch to class $i-1$, i.e. get a lower affinity, the former being much less likely than the latter. In the simulations reported here, 25% of all cells mutate every time step. Out of these 25%, 3% obtain a higher affinity for the antigen.

Cell death is implemented as a shrinking process: cells that do not get rescued are assigned as apoptotic cells. Their target volume decreases two units at each time step. Thus, on average centrocytes die in 15 time steps, and centroblasts die in 20 time steps.

2.4. The parameters

From the selection point of view, the crucial parameters of the model are the minimum interaction time needed to rescue a centrocyte and the contribution that affinity makes to cell adhesion. These parameters are discussed in detail in Section 3.5. The mutation rate, the probability of getting an advantageous mutation, and the lifespan of centroblasts together influence the *all-or-none* behavior, and are discussed in Section 3.4. The recycling probability p_r with which a rescued centrocyte becomes a centroblast, influences the size of a GC. Increasing the recycling probability from 0.2 to 0.6, for example, increases the GC size three-fold. If $p_r = 0$, there is no influx of B cells to the centroblast compartment, and the GC reaction cannot be maintained.

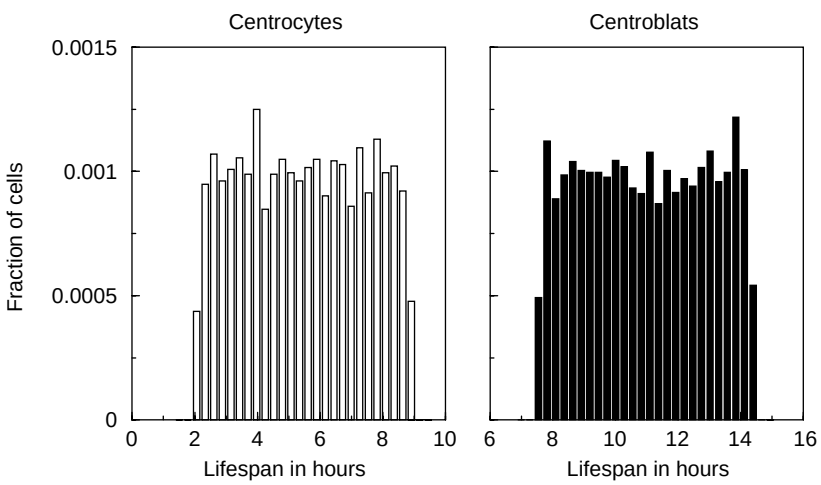

Fig. 4. Distribution of the lifespan of centrocytes (open bars) and centroblasts (filled bars) in a typical simulation. The average lifespan of centroblasts is 12 h and of centrocytes 6 h.

During a simulation time step the CA space is updated by randomly selecting sites in the lattice, and changing the state of the selected sites in order to obtain minimum cell surface energy (see Appendix A for details). These updates allow cells to move, grow, or shrink. After a certain number of these updates, cellular processes like division, death, and phenotype change take place. In the simulation results reported here we have chosen to update the sites 20 times more frequently than the cells, i.e. 50 000 sites are updated in a 50×50 CA per time step. Our results are insensitive to this parameter unless it is too low, e.g. less than 2500, or too high, e.g. more than 500 000. To convert simulation time steps into real time, we measure the average time that elapses between cell divisions in the initial phases of the simulation, i.e. when the space is not yet a limiting factor. In experimental GC reactions, centroblasts have been shown to divide once every 6–7 h (Liu et al., 1991). Using this estimate, 3500 time steps in our simulations correspond to a single day (i.e. each time step corresponds to approximately 25 s). Some parameter values have not been well established experimentally. We have tuned them within reasonable limits to obtain a realistic model behavior (see Table 1).

Table 1
Initial conditions and parameter values

Parameter of initial condition	Value	Ref.
Number of seeder cells per GC	6–8	Kroese et al. (1987)
Maximum proliferation rate of centroblast cells	3.5 day^{-1}	Liu et al. (1991)
Average lifespan of centrocytes	6 h	Cohen et al. (1992)
Average lifespan of centroblasts	12 h	Liu et al. (1994)
Contribution of affinity to cell adhesion for class 0 cells, A_0	0	
Affinity difference between classes, m	10	
Free energy bonds, J	0–10	
Minimum interaction time needed to rescue a centrocyte	3.5 h	
Probability of rescued centrocytes to become a centroblast (p_r)	0.8	
Target volume for centroblasts and memory cells	40 sites	
Target volume for centrocytes (smaller than centroblasts)	30 sites	Brachtel et al. (1996)
Mutation rate per B cell per division	0.25	
Probability of getting an advantageous mutation if mutating	0.03	
CA size	50×50	
Number of sites updated per simulation time step	50 000	

3. Results

3.1. Fast selection of high-affinity mutants in the sorting model

We investigate whether the affinity-based sorting of centrocytes around FDCs ("sorting model", see Section 2.2) allows for fast selection of high-affinity mutants. First, we ask whether fast take-over rates can be reached in biologically realistic parameter regimes. Thus, we neglect mutation and explicitly introduce high-affinity mutants in a sequential manner into established GC reactions to see how fast they take over.

The simulations start with germ line affinity seeders, i.e. with B cells belonging to affinity class 0. When the GC reaction consisting of germ line affinity B cells approaches steady state, we introduce the first high-affinity mutant from affinity class 1. Due to the stochastic nature of the model, a single high-affinity mutant has a "probability" of taking over a GC reaction. For instance, if the mutant fails to reach the FDC, it cannot be selected. Following the terminology introduced by Radmacher et al. (1998), we define a founder mutant as the first mutant in a key lineage which ultimately accounts for domination of the GC. If the first mutant fails to become a founder mutant, we later introduce another mutant of the same affinity class. This process is repeated until one of the mutants becomes the founder mutant, and the GC reaction is dominated by cells from affinity class 1. The same procedure is then repeated for a mutant of the next affinity class. The results of such a simulation are shown in Fig. 5A. The low plateau prior to the fast increase in cell numbers for each affinity class corresponds to the waiting time for the founder mutant; the mutants introduced in this initial phase fail to take over the GC reaction. By the end of the 4-week period, the GC is populated by B cells of affinity class 5. Note from the cell numbers on the vertical axis that the model GC is ten-fold smaller than a typical biological GC (Jacob et al., 1991). It is impossible to obtain larger GCs simply by increasing the lattice size in a two-dimensional (2D) model: even though a large CA could contain ten-fold more cells, centrocytes would fail to reach the FDC in a reasonable time, because cells cannot crawl over other cells. We are currently developing a 3D model with an FDC network, in which centrocytes more easily get access to the FDC.

As the model is highly stochastic, we run 40 simulations, each initialized with different random seeds. For each affinity class we determine the founder mutant. The founder mutant takes over by the S-shaped function described by Eq. (1).

To determine the take-over (growth) rate ρ of the mutant, we perform a linear regression on the fraction of high-affinity cells over the period in which 10–90% of

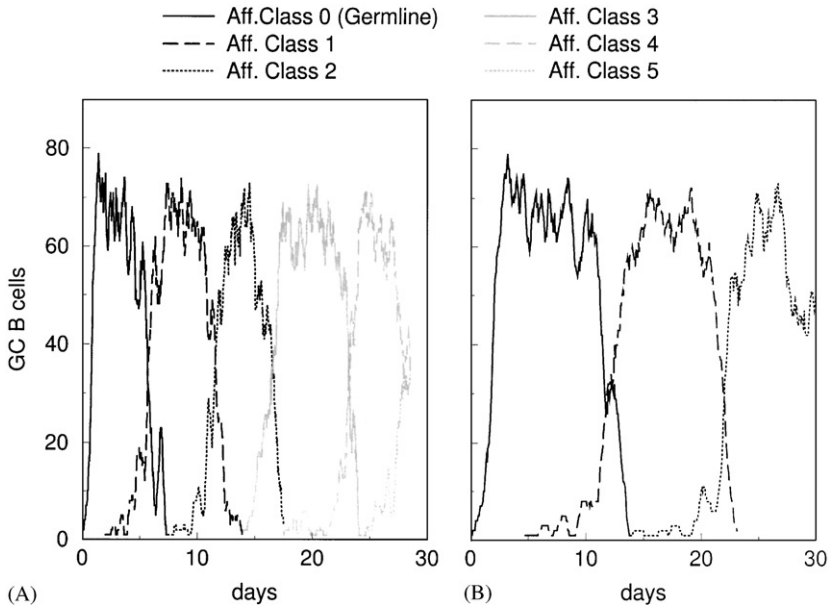

Fig. 5. (A) A typical simulation of the sorting model. A GC reaction starts with a few seeder cells with germ line affinity. After the system has reached steady state we introduce a single high-affinity mutant. This process is repeated each time a GC contains only cells from a single affinity class. (B) Similar simulations in an affinity-proportional selection model where the minimum interaction time with the FDC to get rescued decreases with the affinity. In Fig. 6B, we show the decrease in the minimum interaction time as a function of affinity. The parameters used to obtain these results are given in Table 1.

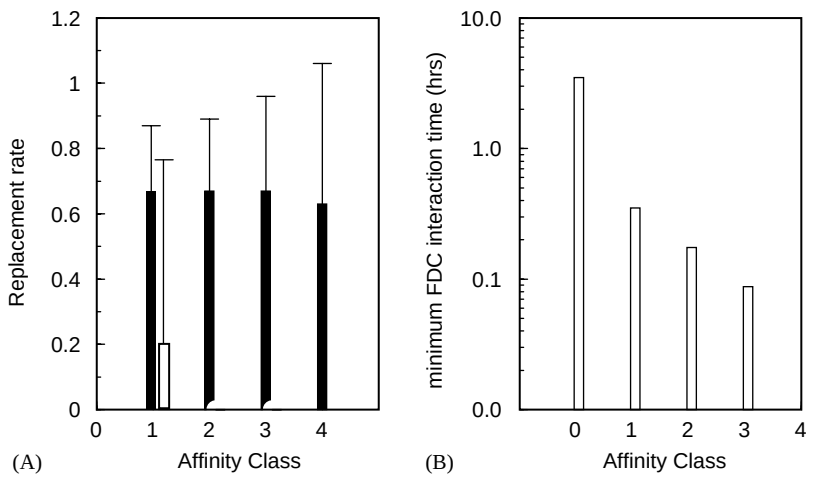

Fig. 6. (A) The replacement rates in the sorting model (filled bars) and in an affinity-proportional selection model incorporating the strong signal hypothesis (open bars). The replacement rate is calculated as explained in the text. In the latter model, the FDC interaction required to obtain survival signals is inversely proportional to the affinity as given in (B). In the sorting model the affinity of a cell does not influence its FDC interaction time or the lifespan of the cell. Each point is an average of 40 simulations, and the error bars give the standard deviations for each affinity class. These results are obtained with the parameter settings given in Table 1. Class 0 represents the germ line B cells.

GC B cells are offspring of the founder high-affinity mutant. The slope of this line defines the take-over rate ρ in Eq. (1) of that mutant. The results are depicted in Fig. 6A. In the sorting model (filled bars) the replacement rate depends only on the affinity differences, not on the absolute affinity values. For example, a mutant from affinity class 3 replaces B cells from affinity class 2 at the same rate as a class one mutant replaces germ line affinity cells.

3.2. Take-over rates in affinity-proportional selection models

For the affinity-proportional selection models there are various mechanisms that increase the proliferation rate or decrease the survival rate of the high-affinity mutants. The results of our ODE model (Section 1) are independent of the mechanism that provides the selective advantage. However, to compare selection

based on sorting of B cells around the FDC, with affinity-proportional selection in our simulation model, we need to choose a specific mechanism. A likely candidate is one where the minimum interaction time with the FDC required to get enough survival signals is inversely proportional to the affinity ("strong signal hypothesis"). Using such a mechanism, a high-affinity mutant would have a higher chance of receiving enough survival signals from the FDC and would spend less time on the FDC, which would allow the cell to proceed more rapidly into cell division. This implies that a high-affinity mutant would have both a higher proliferation rate and a lower apoptosis rate. This mechanism can easily be implemented in our model by (i) excluding the affinity from the adhesion calculation, (i.e. by setting b to zero in Eq. (A.1)), and (ii) making the minimum interaction time with the FDC a function of the affinity, e.g. as given in Fig. 6B. In Fig. 5B, we show a typical time plot of a CA model that incorporates the strong signal hypothesis.

Fig. 5 shows that the sorting model achieves better affinity maturation in 1 month than does an affinity-proportional selection model incorporating the strong signal hypothesis. In agreement with this, the replacement rates in the affinity-proportional selection model are slower than those in the sorting model (see Fig. 6A). We have also compared the sorting model with four other affinity-proportional selection models, where the lifespan of centrocytes or centroblasts increases either linearly or fold-wise (i.e. in powers of 2) with the affinity. In all models, the replacement rates of the higher affinity mutants are lower than in the sorting model (results not shown). In particular, replacing an already established high-affinity mutant by a higher-affinity mutant becomes very difficult (see Fig. 6A, the rate of taking over a GC dominated by cells from affinity class 1 is zero).

3.3. Waiting time for founder mutants

The cautious analysis by Radmacher et al. (1998) shows that high-affinity mutants appear much later than expected from known mutation rates and mutation motifs. For the anti-(4-hydroxy-3-nitrophenyl) acetyl (NP) response, the waiting time for the key mutant with one mutation at position 33 is 8.3 days (Radmacher et al., 1998). This waiting time strongly contradicts with the expected time of 2.3 days. Apparently, an average of 2.6 mutants arise, but do not take root in GCs before the *founder* mutant arrives. Radmacher et al. (1998) suggested several mechanisms that might cause the failure of early high-affinity mutants to take over, e.g. a low chance of finding the right T cell, or fast emigration from the GC.

In our hybrid GC not every high-affinity mutant takes over a GC, because the cellular processes are highly stochastic. The chance of reaching the FDC and being rescued is proportional to the number of offspring (i.e. clone size). How many offspring a high-affinity mutant generates depends on where and when in the life cycle the advantageous mutation occurs. A centroblast acquiring an affinity-increasing mutation late in the life cycle is expected to have a small number of offspring before becoming a centrocyte. Additionally, the space available around a centroblast affects the number of offspring it gets.

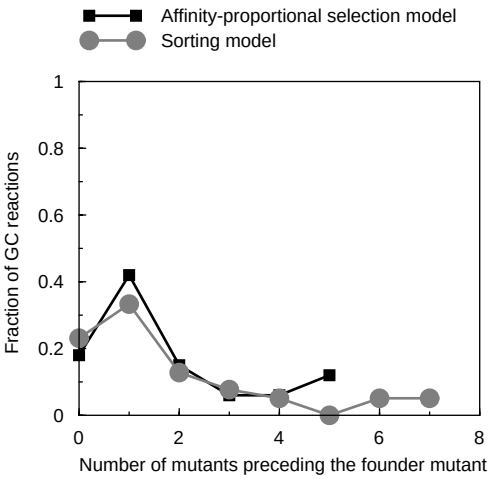

Fig. 7. Distribution of the number of mutants preceding the founder mutant for affinity class 1, calculated over 40 simulations for each model. The mean number of mutants preceding the founder mutant is 1.6 in the sorting model and 1.7 in the affinity-proportional selection model (implementing the strong signal hypothesis). Very similar numbers are obtained for other affinity classes in the sorting model.

To study the average number of mutants preceding a founder mutant we run 40 simulations. In Fig. 7, we plot the fraction of simulations in which the first, second, third etc. high-affinity mutant becomes the founder mutant. The mean number of mutants preceding the founder mutant in the sorting model is 1.6 mutants, which is still lower than the results of Radmacher et al. (1998). Similar results are obtained for the affinity-proportional model incorporating the strong signal hypothesis (the mean number of mutants preceding the founder mutant being 1.7 mutants).

3.4. All-or-none behavior

GCs induced during immune responses to haptens rarely contain both high- and low-affinity B cells (Radmacher et al., 1998) Instead, an *all-or-none* behavior is typically observed, i.e. a GC is either dominated by a high-affinity mutant or does not contain any high-affinity mutant at all. In Fig. 8 (open squares), we plot the available data for the anti-NP (Radmacher et al., 1998) and anti-2-phenyl-oxazolone (phOx) (Berek et al., 1991; Ziegner et al., 1994) responses. About 60% of the GCs analysed have no high-affinity mutants at all.

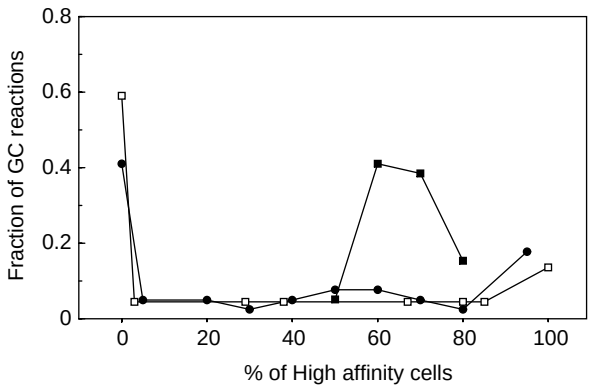

Fig. 8. Distribution of high-affinity cells in GCs analysed for the anti-NP (Radmacher et al., 1998) and the anti-phOx (Berek et al., 1991; Ziegner et al., 1994) response (total of 22 GCs, open squares) and in our simulations (total of 40 GCs). The simulations are run for 14 days, the mutation rate per cell division is 25% and the probability of getting an advantageous mutation is set to 3%. The filled circles show the results of the sorting model, whereas the filled squares show the results obtained with affinity-proportional selection model (implementing the strong signal hypothesis). Before day 14, the percentage of GCs that do not contain any high affinity mutants is higher, whereas after 14 days, more GCs contain high-affinity mutants only.

There are very few mixed GCs, and the remaining GCs have high-affinity mutants only.

To test whether the sorting model is able to simulate such an *all-or-none* behavior, we allow cells to mutate during cell division. The mutation rate per cell division is 25% and if a mutation occurs, the probability of getting an advantageous mutation is 3%. We again run 40 simulations. The distribution of high-affinity mutants in the model GCs is shown in Fig. 8 (sorting model: filled circles, affinity-proportional model: filled squares). The sorting model shows a striking agreement to the empirical data. These results have to be interpreted with some caution, however. Since our model GC contains only 10% of the number of cells in a real GC, the stochastic effects are probably too large in our model. The 3D model, that we are currently developing will help to study this matter further. The affinity-proportional selection model results in mixed GCs in a large range of parameters (see Fig. 8). The main reason for the failure of the affinity-proportional selection models to yield the *all-or-none* behavior is the slow take over rates of higher affinity mutants (see Fig. 6A).

The results depicted in Fig. 8 for the sorting model can only be obtained if the proliferation, mutation and selection cycle is short. If the centroblasts make several cell divisions without being selected, they accumulate disadvantageous mutations, resulting in very poor affinity maturation. Almost all GCs then contain low-affinity cells. This behavior could be an artifact of the high mutation rate per division (0.25) that we use in the simulations. Our parameters allow centroblasts to undergo on average two cell divisions before converting to the centrocyte stage.

It is an open question whether a GC containing 100% high-affinity cells can be found *in vivo* because high mutation rates cause decay of high affinity cells. This mutational erosion is visible in our simulation model: we can simulate an almost *all-or-none* behavior, in which GCs consist mainly of high-affinity cells but also contain 5% low-affinity cells.

3.5. Crucial parameters

Only few of the molecules regulating the adhesion between a B cell and an FDC have been identified (Airas and Jalkanen, 1996; Pals et al., 1998). To our knowledge there are for example no good estimates of the contribution of affinity to adhesion energy. In other words, the value A_i for a mutant from affinity class i (Eq. (A.1) of Appendix A) is unknown. The results in Fig. 9A depict the average replacement rate in five simulations for a range of A_1 values. We plot the replacement rates of a class 1 mutant in a GC established by germ line affinity B cells (Fig. 6A implies that the replacement rates should be similar for higher-affinity mutants). If affinity makes a small contribution to the adhesion, i.e. for low values of A_1, the take-over is slow. This parameter regime results in mixed GCs, rather than the *all-or-none* behavior. Once A_1 is sufficiently large, e.g. $A_1 > 8$, increasing A_1 does not affect the replacement rates drastically. If the A_1 value is very large ($A_1 \gg 20$), the cellular adhesion overrules the volume constraints, and cells lose their shape.

Another crucial parameter of the model is the minimum interaction time with the FDC required for rescuing a centrocyte. In the sorting model, we assume that the minimum interaction time is independent of the affinity. Obviously, if this time is very short, high-affinity cells spend very little time on the surface of the FDC and can hardly block the survival signals for other cells. The effect of this parameter on the replacement rate is shown in Fig. 9B. Short interaction times result in very low replacement rates. The *winner-takes-all* behavior is realized only when the survival signals are delivered over a few hours, which is in agreement with *in vivo* estimates for this parameter (MacLennan, 1994).

4. Discussion

Two processes bring about efficient affinity maturation of humoral immune responses. First, hypermutation generates a large number of mutations and second, mutants producing high-affinity antibodies have to be selected efficiently (Radmacher et al., 1998). In the earlier models of affinity maturation, selection of high-affinity mutants is typically proportional to their-affinity, either via increased proliferation rates or via decreased apoptosis rates of high-affinity cells

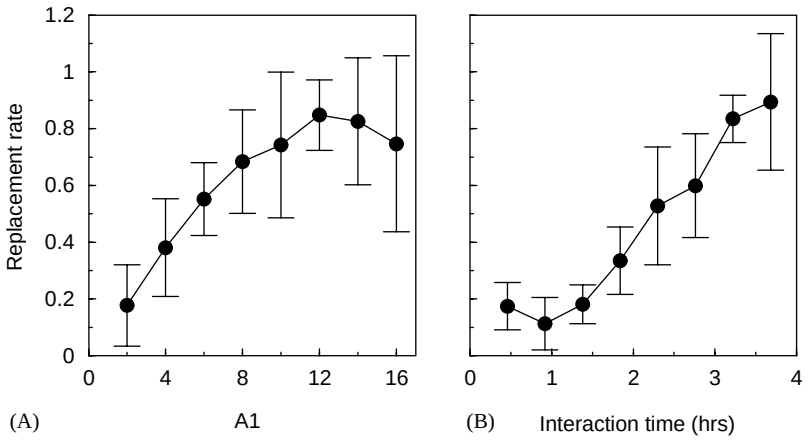

Fig. 9. (A) The effect of the contribution of affinity to cellular adhesion A_i on B cell competition. (B) The effect of the interaction time with FDCs on B cell competition. Each data point is the mean of five simulations, and the error bars show the standard deviations. In both panels, the rate of replacement of germ line B cells by a class 1 mutant is shown.

(Kepler and Perelson, 1993b; Oprea and Perelson, 1997). We have shown that, unless unreasonably high proliferation rates or survival rates are used, these mechanisms are not able to explain the observed rapid replacement of low-affinity cells (see Section 1). To solve this problem, we proposed a novel mechanism where B cells sort on the FDC surface according to their affinities. We have shown that such a mechanism results in *winner-takes-all* and *all-or-none* behavior.

Comparing the new model with affinity-proportional selection models, one has to be cautious about the choice of the mechanisms and the parameters, before making a general statement. Our analytic results of Section 1 are valid for affinity-proportional selection mechanisms in general because the competitive functions we use are not specific, but the results obtained with the simulation model are dependent on our specific choice of the mechanisms and parameters. With more extreme parameters, e.g. if high-affinity mutants get enough survival signals in seconds, it is possible to decrease the difference between the affinity-proportional selection model and the sorting model for the first high-affinity mutant, but consecutive mutants are always hard to be replaced if there is only affinity-proportional selection. There is also no biological evidence supporting such extreme parameter regimes.

In the sorting model, the replacement rate (see Fig. 6) is lower than the observed 4 per day (Radmacher et al., 1998). This could be due to our conservative scaling of time: When converting simulation time steps to real time, we measured how long the cell division takes in the early phase of the simulations (when space is not yet a limiting factor). Using this value we calculated that each time step in the model corresponds to 25 s in real time. However, later in the simulations, when a GC is filled with B cells, the centroblast division rate slows down due to spatial competition. In the later phase, the division rate is 3–4 times slower than during the early phase. Using the later cell division time, a simulation time step would correspond to 6 s, which results in replacement rates close to 4 per day (results not shown). The main result in Fig. 6 is the fact that under the *same* conditions, e.g. where cells compete for space and are moving with the same speed, affinity-based cell sorting produces faster take-over rates than affinity-proportional selection.

It is difficult to verify experimentally how much a B cell's affinity for antigen contributes to its adhesion to an FDC. However, we show in Fig. 9A that the precise value of this contribution is not important, provided it plays a sufficient role (i.e. $A > 8$). Demonstrating that high-affinity cells have significantly higher adhesion to FDCs than low-affinity cells would be sufficient to support the adhesion-based selection mechanism. Obviously, if the affinity of cells hardly contributes to their adhesion to FDCs, i.e. if $A < 8$, the *winner-takes-all* and *all-or-none* behavior that we report would not be valid. Some other simulation results can be tested more easily. For example, Fig. 9B predicts that the minimum interaction time needed to receive survival signals should affect the efficiency of affinity maturation. Some molecules like 8D6 Ag (Li et al., 2000) were shown to transmit survival/growth signals to B cells. Experiments with knock-out (or knock-in) animals where the density of such survival signals decreases (or increases) would allow one to test our prediction. We show that the current estimates of the minimum interaction time, amounting to a few hours (MacLennan, 1994), give rise to efficient affinity maturation (see Fig. 9B).

T cells in the GC also play a role in the selection of high-affinity mutants (Choe et al., 2000; Lindhout et al., 1997; Manser et al., 1998; Yellin et al., 1994). Our model focuses on FDC-based selection of mutants. However,

T-cell-based selection would be different from FDC-based selection, because FDCs are large stationary cells, whereas T cells are small and mobile. In a spatial model, these differences might play a role. In an FDC-based selection model, the limiting factor, i.e. space on the FDC surface, is always constant. This is not the case for T-cell-based selection, especially if T cells proliferate after interacting with high-affinity B cells.

Somatic mutations can take place either during cell division (Cascalho et al., 1998; Rogerson et al., 1991) or during transcription, i.e. when a cell starts to re-express surface immunoglobulin (converting to the centrocyte phenotype) (Peters and Storb, 1996; Storb et al., 1998). Here, we implement mutations during cell division. In a recent mathematical model, it has been shown that mutations during the transcription phase result in better affinity maturation (Oprea et al., 2000). We also observe this in our simulations: if affinity-altering mutations occur during the transcription phase, the *all-or-none* behavior of Section 3.4 becomes more pronounced (results not shown).

The *winner-takes-all* behavior is not limited to competition of B cell mutants. Early in GC reactions there is also very strong competition between seeders (Chen et al., 2000). Furthermore, post-GC antibody-forming cells in the bone marrow may compete directly for activation by antigen. There is good evidence that this selection plays a major role in the post-GC maturation of humoral responses (Takahashi et al., 1998). *Winner-takes-all* behavior is also observed in many other ecological systems (see e.g. Krause, 1994 for a review on lek mating systems).

Several conventional affinity-proportional selection models have been used to study affinity maturation in germinal center reactions (Kepler and Perelson, 1993a, b; Kleinstein and Singh, 2001; Oprea and Perelson, 1997; Oprea et al., 2000). We here show that these models are poor at simulating two general features of affinity maturation, namely *winner-takes-all* and *all-or-none* behavior. As an alternative to these selection mechanisms we propose a novel mechanism where centrocytes are sorted on FDCs according to their affinity. Our results obtained with a spatial model suggest that this adhesion-based selection mechanism is much more likely to generate the affinity maturation observed *in vivo*.

Acknowledgements

This work was initiated by Berend Snel. This paper has benefited greatly from critical comments by Ludo Pagie, Vincent DeTours, José Borghans and Paulien Hogeweg. CK is supported by grant 809.37.009 of the Dutch Science Foundation.

Appendix A

We define the surface energy as a Hamiltonian. For each lattice site on the surface of a cell surface, we calculate the change in Hamiltonian to decide whether or not the cell can grow to an adjacent site. The Hamiltonian is given as

$$H = \sum J_{cell,cell} + \sum J_{cell,m} - bA_i + \lambda(v - V)^2 + \mu C, \quad \text{(A.1)}$$

where the first term represents dimensionless free energy bonds with neighboring cells, the magnitude being dependent on both cell types (Glazier and Graner 1993; Graner and Glazier, 1992). The bond energy between a cell and the medium is given by $J_{cell,m}$. All J values are positive and are less than 10. Centrocytes have more adhesion to the FDC than centroblasts and memory cells. All cell types have the same bond energy with the medium. The contribution of the affinity of a B cell of class i to its total surface energy is given by A_i. Obviously, this is only true when a B cell expresses surface immunoglobulin and is in contact with the antigen, i.e.

$$b = \begin{cases} 1 & \text{when a controcyte is in contact with an FDC} \\ 0 & \text{otherwise.} \end{cases} \quad \text{(A.2)}$$

The affinity contributions to surface energy change with the affinity class, i.e. $A_i = A_0 + m \times i$, where A_0 is the affinity contribution for class 0 and m is affinity difference between classes.

Since a cell could minimize its surface free energy by shrinking to a volume of zero, we add a volume constraint (i.e. the fourth term in Eq. (A.1)) to the free energy calculations, so that each cell keeps its actual volume v close to its target volume V. The parameter λ defines the "inelasticity". In the simulations reported here we use $\lambda = 0.1$.

Finally, chemotactic signals affect the cell movement. We assume that only the FDC produces chemotactic signals (Bouzahzah et al., 1996), C. Each cell type has a certain sensitivity to chemotaxis (i.e. μ is a parameter that is cell-type dependent). We use a simple chemotactic gradient, that decreases linearly with the distance from the FDC.

ΔH is the change in H when a lattice site j is copied to i. The probability of making such an update is defined as a Boltzmann distribution, i.e.

$$p = \begin{cases} 1 & \text{if } \Delta H < \theta = 0, \\ e^{-\Delta H/T} & \text{otherwise,} \end{cases}$$

where T is the default mobility of cells, and p is the probability of copying lattice site j to i. When an update occurs, e.g. when a cell grows and a neighbor cell

shrinks, both cells change their surface energy. Thus, ΔH is calculated by taking the changes of the surface energy of both cells into account. Throughout the CA, this process is implemented for all sites on the surface of cells. This results in minimization of the total surface energy of *all* GC cells. In the simulations reported here we use $T = 20$.

References

Airas, L., Jalkanen, S., 1996. CD73 mediates adhesion of B cells to follicular dendritic cells. Blood 88, 1755–1764.

Berek, C., Milstein, C., 1987. Mutation drift and repertoire shift in the maturation of the immune response. Immunol. Rev. 96, 23–41.

Berek, C., Berger, A., Apel, M., 1991. Maturation of the immune response in germinal centers. Cell 67, 1121–1129.

Betz, A.G., Neuberger, M.S., Milstein, C., 1993. Discriminating intrinsic and antigen-selected mutational hotspots in immunoglobulin V genes. Immunol. Today 14, 405–411.

Bouzahzah, F., Antoine, N., Simar, L., Heinen, E., 1996. Chemotaxis-promoting and adhesion properties of human tonsillar follicular dendritic cell clusters. Res. Immunol. 147, 165–173.

Brachtel, E.F., Washiyama, M., Johnson, G.D., Tenner-Racz, K., Racz, P., MacLennan, I.C., 1996. Differences in the germinal centres of palatine tonsils and lymph nodes. Scand. J. Immunol. 43, 239–247.

Casamayor-Palleja, M., Khan, M., MacLennan, I.C., 1995. A subset of $CD4^+$ memory T cells contains preformed CD40 ligand that is rapidly but transiently expressed on their surface after activation through the T cell receptor complex. J. Exp. Med. 181, 1293–1301.

Cascalho, M., Wong, J., Steinberg, C., Wabl, M., 1998. Mismatch repair co-opted by hypermutation. Science 279, 1207–1210.

Chen, Z., Koralov, S.B., Gendelman, M., Carroll, M.C., Kelsoe, G., 2000. Humoral immune responses in $Cr2^{-/-}$ mice: enhanced affinity maturation but impaired antibody persistence. J. Immunol. 164, 4522–4532.

Choe, J., Li, L., Zhang, X., Gregory, C.D., Choi, Y.S., 2000. Distinct role of follicular dendritic cells and T cells in the proliferation, differentiation, and apoptosis of a centroblast cell line, L3055. J. Immunol. 164, 56–63.

Cohen, J.J., Duke, R.C., Fadok, V.A., Sellins, K.S., 1992. Apoptosis and programmed cell death in immunity. Annu. Rev. Immunol. 10, 267–293.

Glazier, J.A., Graner, F., 1993. Simulation of the differential adhesion driven rearrangement of biological cells. Phys. Rev. E 47, 2128–2154.

Graner, F., Glazier, J.A., 1992. Simulation of biological cell sorting using a two-dimensional extended Potts model. Phys. Rev. Lett. 69, 2013–2016.

Hogeweg, P., 2000a. Evolving mechanisms of morphogenesis: on the interplay between differential adhesion and cell differentiation. J. theor. Biol. 203, 317–333.

Hogeweg, P., 2000b. Shapes in the shadow: evolutionary dynamics of morphogenesis. Artif. Life. 6, 85–101.

Jacob, J., Kassir, R., Kelsoe, G., 1991. In situ studies of the primary immune response to (4-hydroxy-3-nitrophenyl) acetyl I. The architecture and dynamics of responding cell populations. J. Exp. Med. 173, 1165–1175.

Jiang, Y., Levine, H., Glazier, J., 1998. Possible cooperation of differential adhesion and chemotaxis in mound formation of Dictyostelium. Biophys. J. 75, 2615–2625.

Kelsoe, G., 1996. Life and death in germinal centers (redux). Immunity 4, 107–111.

Kelsoe, G., 1999. V(D)J hypermutation and receptor revision: coloring outside the lines. Curr. Opin. Immunol. 11, 70–75.

Kepler, T.B., Perelson, A.S., 1993a. Cyclic re-entry of germinal center B cells and the efficiency of affinity maturation. Immunol. Today 14, 412–415.

Kepler, T.B., Perelson, A.S., 1993b. Somatic hypermutation in B cells: an optimal control treatment. J. theor. Biol. 164, 37–64.

Klein, U., Goossens, T., Fischer, M., Kanzler, H., Braeuninger, A., Rajewsky, K., Kuppers, R., 1998. Somatic hypermutation in normal and transformed human B cells. Immunol. Rev. 162, 261–280.

Kleinstein, S.H., Singh, J.P., 2001. Toward quantitative simulation of germinal center dynamics: biological and modeling insights from experimental validation. J. theor. Biol. 211, 253–275.

Koopman, G., Keehnen, R.M., Lindhout, E., Zhou, D.F., De Groot, C., Pals, S.T., 1997. Germinal center B cells rescued from apoptosis by CD40 ligation or attachment to follicular dendritic cells, but not by engagement of surface immunoglobulin or adhesion receptors, become resistant to CD95- induced apoptosis. Eur. J. Immunol. 27, 1–7.

Krause, J., 1994. Differential fitness returns in relation to spatial position in groups. Biol. Rev. Camb. Philos. Soc. 69, 187–206.

Kroese, F.G., Wubbena, A.S., Seijen, H.G., Nieuwenhuis, P., 1987. Germinal centers develop oligoclonally. Eur. J. Immunol. 17, 1069–1072.

Legler, D.F., Loetscher, M., Roos, R.S., Clark-Lewis, I., Baggiolini, M., Moser, B., 1998. B cell-attracting chemokine 1, a human CXC chemokine expressed in lymphoid tissues, selectively attracts B lymphocytes via BLR1/CXCR5. J. Exp. Med. 187, 655–660.

Li, L., Zhang, X., Kovacic, S., Long, A.J., Bourque, K., Wood, C.R., Choi, Y.S., 2000. Identification of a human follicular dendritic cell molecule that stimulates germinal center B cell growth. J. Exp. Med. 191, 1077–1084.

Lindhout, E., Koopman, G., Pals, S.T., De Groot, C., 1997. Triple check for antigen specificity of B cells during germinal centre reactions. Immunol. Today 18, 573–577.

Liu, Y.J., Banchereau, J., 1997. Regulation of B-cell commitment to plasma cells or to memory B cells. Semin. Immunol. 9, 235–240.

Liu, Y.J., Zhang, J., Lane, P.J., Chan, E.Y., MacLennan, I.C., 1991. Sites of specific B cell activation in primary and secondary responses to T cell-dependent and T cell-independent antigens. Eur. J. Immunol. 21, 2951–2962.

Liu, Y.J., Barthelemy, C., de Bouteiller, O., Banchereau, J., 1994. The differences in survival and phenotype between centroblasts and centrocytes. Adv. Exp. Med. Biol. 355, 213–218.

MacLennan, I.C., 1994. Germinal centers. Annu. Rev. Immunol. 12, 117–139.

Manser, T., Tumas-Brundage, K.M., Casson, L.P., Giusti, A.M., Hande, S., Notidis, E., Vora, K.A., 1998. The roles of antibody variable region hypermutation and selection in the development of the memory B-cell compartment. Immunol. Rev. 162, 183–196.

Maree, A.F., Hogeweg, P., 2001. How amoeboids self-organize into a fruiting body: multicellular coordination in *dictyostelium discoideum*. Proc. Natl Acad. Sci. 98, 3879–3883.

Maree, A.F., Panfilov, A.V., Hogeweg, P., 1999. Migration and thermo-taxis of dictyostelium discoideum slugs, a model study. J. theor. Biol. 199, 297–309.

Maree, A.F., Keulen, W., Boucher, C.A., De Boer, R.J, 2000. Estimating relative fitness in viral competition experiments. J. Virol. 74, 11067–11072.

Mombach, J.C., Glazier, J.A., 1996. Single cell motion in aggregates of embryonic cells. Phys. Rev. Lett. 76, 3032–3035.

Mombach, J.C., Glazier, J.A., Raphael, R.C., Zajac, M., 1995. Quantitative comparison between differential adhesion models and cell sorting in the presence and absence of fluctuations. Phys. Rev. Lett. 75, 2244–2247.

Oprea, M., Perelson, A.S., 1997. Somatic mutation leads to efficient affinity maturation when centrocytes recycle back to centroblasts. J. Immunol. 158, 5155–5162.

Oprea, M., Van Nimwegen, E., Perelson, A.S., 2000. Dynamics of one-pass germinal center models: implications for affinity maturation. Bull. Math. Biol. 62, 121–153.

Pals, S.T., Taher, T.E., Van der Voort, R., Smit, L., Keehnen, R.M., 1998. Regulation of adhesion and migration in the germinal center microenvironment. Cell. Adhes. Commun. 6, 111–116.

Peters, A., Storb, U., 1996. Somatic hypermutation of immunoglobulin genes is linked to transcription initiation. Immunity 4, 57–65.

Przylepa, J., Himes, C., Kelsoe, G., 1998. Lymphocyte development and selection in germinal centers. Curr. Top. Microbiol. Immunol. 229, 85–104.

Radmacher, M.D., Kelsoe, G., Kepler, T.B., 1998. Predicted and inferred waiting times for key mutations in the germinal centre reaction: evidence for stochasticity in selection. Immunol. Cell. Biol. 76, 373–381.

Ridderstad, A., Tarlinton, D.M., 1998. Kinetics of establishing the memory B cell population as revealed by CD38 expression. J. Immunol. 160, 4688–4695.

Rogerson, B., Hackett Jr., J., Peters, A., Haasch, D., Storb, U., 1991. Mutation pattern of immunoglobulin transgenes is compatible with a model of somatic hypermutation in which targeting of the mutator is linked to the direction of DNA replication. EMBO J. 10, 4331–4341.

Savill, N.J., Hogeweg, P., 1997. Modeling morphogenesis: from single cells to crawling slugs. J. theor. Biol. 184, 229–235.

Steinberg, M.S., 1970. Does differential adhesion govern self-assembly processes in histogenesis? Equilibrium configurations and the emergence of a hierarchy among populations of embryonic cells. J. Exp. Zool. 173, 395–433.

Storb, U., Peters, A., Klotz, E., Kim, N., Shen, H.M., Kage, K., Rogerson, B., Martin, T.E., 1998. Somatic hypermutation of immunoglobulin genes is linked to transcription. Curr. Top. Microbiol. Immunol. 229, 11–19.

Takahashi, Y., Dutta, P.R., Cerasoli, D.M., Kelsoe, G., 1998. In situ studies of the primary immune response to (4-hydroxy-3-nitrophenyl) acetyl. V. Affinity maturation develops in two stages of clonal selection. J. Exp. Med. 187, 885–895.

Tarlinton, D., 1998. Germinal centers: form and function. Curr. Opin. lmmunol. 10, 245–251.

Wabl, M., Cascalho, M., Steinberg, C., 1999. Hypermutation in antibody affinity maturation. Curr. Opin. Immunol. 11, 186–189.

Wiens, G.D., Roberts, V.A., Whitcomb, E.A., O'Hare, T., Stenzel-Poore, M.P., Rittenberg, M.B., 1998. Harmful somatic mutations: lessons from the dark side. Immunol. Rev. 162, 197–209.

Yelamos, J., Klix, N., Goyenechea, B., Lozano, F., Chui, Y.L., Gonzalez Fernandez, A., Pannell, R., Neuberger, M.S., Milstein, C., 1995. Targeting of non-Ig sequences in place of the V segment by somatic hypermutation. Nature 376, 225–229.

Yellin, M.J., Sinning, J., Covey, L.R., Sherman, W., Lee, J.J., Glickman-Nir, E., Sippel, K.C., Rogers, J., Cleary, A.M., Parker, M., et al., 1994. T lymphocyte T cell-B cell-activating molecule/CD40-L molecules induce normal B cells or chronic lymphocytic leukemia B cells to express CD80 (B7/BB-1) and enhance their costimulatory activity. J. Immunol. 153, 666–674.

Ziegner, M., Steinhauser, G., Berek, C., 1994. Development of antibody diversity in single germinal centers: selective expansion of high-affinity variants. Eur. J. Immunol. 24, 2393–2400.